Journal of Materials Science & Nanotechnology
Volume 6 | Issue 2
ISSN: 2348-9812

Research Article Open Access

The Influence of Sodium on the Characterization of $Cu(In,Ga)Se_2$ Thin Films Prepared by Three-Stage Deposition Process

Jseng YY[*1,2], Chao CJ[2], Sung HH[3], and Chen TC[3]

[1]National Chung-Shan Institute of Science and Technology, Longtan Dist, Taoyuan, Taiwan
[2]Department of Industrial and Systems Engineering, Chung Yuan Christian University, Taoyuan, Taiwan
[3]GeniRay Technology Corporation, Xinzhuang Dist, New Taipei City, Taiwan

[*]**Corresponding author:** Jseng YY, National Chung-Shan Institute of Science and Technology, No.481, 6th Neighborhood, Sec. Jia'an, Zhongzheng Road, Longtan District, Taoyuan 32546, Taiwan, Tel: 910753930, E-mail: yen913013@yahoo.com.tw

Citation: Jseng YY, Chao CJ, Sung HH, Chen TC (2018) The Influence of Sodium on the Characterization of $Cu(In,Ga)Se_2$ Thin Films Prepared by Three-Stage Deposition Process. J Mater Sci Nanotechnol 6(2): 203

Abstract

The objective of this work is to investigate the influence of sodium on the characteristics of $Cu(In,Ga)Se_2$ (CIGS) thin films prepared by a three-stage deposition process with a MoNa back contact, in comparison to Mo/SLG. The XRD results show that all the CIGS thin films deposited onto Mo/SLG substrates have the (112) preferred orientation, rather than the (220/204) orientation of CIGS deposited onto Na-free substrates. As the thickness of the MoNa increases, the (220/204) orientation becomes more common in the CIGS thin films due to the surfactant effect of the sodium which can reduce the surface free energy during the growth process. A stronger Ga gradient and a decrease of grain size near the back contact are observed when the Na content increases. Raman analysis reveals that all the CIGS thin films exhibit a single peak without the occurrence of an OVC compound. The Raman peaks of the absorber layers shift from 174 cm-1 to 171 cm-1 as a result of the formation of a more stable $NaInSe_2$ compound by the replacement of Cu vacancy sites by Na. The conversion efficiencies of CIGS solar cells deposited on SLG/Mo and Na-free glass/Mo/MoNa(200nm)/Mo are 13.71% and 14.24%, respectively.

Keywords: $Cu(In,Ga)Se_2$; Three-stage Deposition Process; MoNa; Back Contact

Introduction

The advantages of $Cu(In,Ga)Se_2$(CIGS), their direct band gap, high light absorption coefficient (1×10^5 cm^{-1}), controllable band gap, etc., have made it one of the most attractive thin films for solar cells with a conversion efficiency of over 20% [1,2]. Nowadays, it has been demonstrated that the insufficient-copper CIGS thin films prepared by the three-stage deposition process can achieve a high conversion efficiency due to the lowering of the defect formation energy (less than 1eV) [3,4]. A composite defect structure ($2V_{Cu}^{-} + In_{Cu}^{2+}$) that has a negative value of formation energy spontaneously appears as a consequence of order vacancy compounds (OVCs) at the surface, which can lead to Cd ion diffusion into the surface of the absorber layer to produce a buried homo-junction during the chemical bath deposition process [5]. Meanwhile, improving the open-circuit voltage and short-circuit current densities of solar devices during the three-stage deposition process depends upon the formation of the depth-profile gallium gradient [6]. The key for the development of high-efficiency devices is to effectively control the gallium gradient [7,8].

Furthermore, sodium supplied in the roll-to-roll manufacturing process with a non-sodium based flexible substrate, such as stainless steel, titanium or polymer, plays a very important role in the development of high efficiency devices [9,10]. The effects of the addition of alkali metal are summarized as follows: (1) an increase in the hole carrier concentration and electric conductivity of the absorber layers can enhance the open-circuit voltage and fill factor of solar devices; (2) the preferred orientation of the absorber layers has an influence on the Cd ion diffusion; (3) the amount of sodium added affects the grain size in the absorber layer; (4) gallium diffusion is inhibited by the sodium during the three-stage deposition process [11-19]. The most common way to add sodium is by deposition of NaF fluorides through an evaporation process [14,20-22]. However, a CIGS solar cell fabricated using a NaF content lower than that of soda-lime glass exhibits insufficiencies effect due to avoiding the substrate adhesion problem as well as the survival phenomenon at low processing temperatures or high NaF content. It should be mentioned that CIGS solar cells may achieve an efficiency of up to 16.6% when using a sodium-doped molybdenum target (MoNa) as the sodium source [23]. In this study, the preferred orientation of the structure, surface morphology and characteristics of the absorber layers of devices prepared by the three-stage deposition process with different thicknesses of MoNa back contacts are investigated.

Experimental Procedure

CIGS absorber layers were deposited on soda-lime glass (SLG) and silicon wafers coated with approximately 100 nm silica and prepared by plasma enhanced chemical vapor deposition (plasma-enhanced chemical vapor deposition, PECVD). The commercially available sputtering targets with sodium concentrations of 10 at% were used. The sodium was incorporated onto the Mo target material in the form of sodiummolybdate (Na_2MoO_4), therefore the amount of oxygen increased with an increase in the thickness of the MoNa. Two series of back contact layers were fabricated on SLG substrates of 1000 nm and on silicon wafers with a sandwich design with upper and lower layers of 500 nm, respectively, and intermediate MoNa layers of 0 nm, 100 nm and 200 nm. The resistance for the MoNa back contacts with different thicknesses can be maintained at 40-50μΩcm.

The absorber layers were fabricated by a three-stage deposition process using an evaporation system equipped with an X-ray fluorescence (XRF) detector. During the first stage, In, Ga and Se were co-evaporated onto the substrates to form the $(In,Ga)_2Se_3$ film at a substrate temperature of 350 ˚C. At the end of second stage, the films were exposed with a flux of Cu and Se at a substrate temperature of 550 ˚C to produce a slightly Cu-rich composition, Cu / (In +Ga)=1.2 ~ 1.22. In the third stage, the addition of In Ga, and Se flux were supplied to change the Cu-rich to a slightly (InGa)-rich composition. The composition of all the absorber layers was Cu / (In +Ga)= 0.80 and Ga / (In +Ga)= 0.3, with a thickness of about 1.5 - 1.6 um. The crystal structure and morphology of the absorber layers were investigated by X-ray diffraction (XRD) using a CuKα radiation source (λ=1.5406 Å) and field emission scanning electron microscopy (FESEM). Characterization of the absorber layers was performed by Raman spectrometry with a laser source with a wave length of 488 nm.

Devices with the CIGS films were fabricated by deposition in a chemical bath of a 50 nm CdS buffer layer, an RF sputtered 70 nm i-ZnO, a DC sputtered 350 nm AZO and a DC sputtered 50 nm Ni/2 um Al front contact grid, in order to facilitate current collection. Individual solar cells with an area of 0.5 cm2 were characterized using an AM 1.5 solar simulator.

Results and Discussion

Figure 1 shows that the structure of all absorber layers is a chalcopyrite phase with XRD peaks of (112), (103), (211), (220/204), (312/116), (224), (400/008), (316/332). It can be observed that the absorber layer deposited on SLG exhibited a (112) preferred orientation, in contrast to the (220/204) orientation appearing on the MoNa back contact. The degree of the preferred orientation of the absorber layers was quantified. In this study, 3 peaks of (112), (220/204) and (312/116) were used for calculation, with the ratio of the integrated intensities of selected peaks to the sum of all peaks in a scanned range, as shown in Figure 2. In general, the (112) preferred orientation would form in the Cu-poor absorber layers in order to reduce the surface free energy under the formation of Cu vacancies V_{Cu} and In_{Cu} antisite defects [11,13,14]. It has been reported that the ratio of (006) plane and (003) plane in $(In,Ga)_2Se_3$ films, appearing at XRD peak positions of approximately 27° and 46°, may tailor the (112) and (220/204) preferred orientations during the absorber layer growth process [15]. However, it is clear that the ratio of (220/204) can be improved from 0.44 to 0.5 as well as a decrease in (112) orientation from 0.36 to 0.32 as the by increasing the MoNa layer thickness from o nm to 100nm. There are models reported in the literature that describe the growth mechanism of CIGS absorber layers using a three-stage deposition process: via a vapor-liquid-solid mechanism and the existence of a semi-liquid Cu-Se phase that forms at temperatures over 523 ˚C. The Cu vacancies provide a diffusion path to obtain a quality material with large grains [24-26]. Typical Na concentrations found in such CIGS layers are of the order of 0.1 at% [27-32]. Therefore, the use of the proper Na content to produce a surfactant effect diffusing through the semi-liquid Cu-Se phase and arriving at the Na-passivated surface of a CIGS grain may not be incorporated into the CIGS crystal straight away. It is indicated that the surfactant effect is beneficial to the growth of the a (220/204) preferred orientation for the formation of the lowest surface energy, instead of the (112) preferred orientation under the excess Na content which acts as an obstacle that limits the inter-diffusion of In and Ga atoms. Figure 3 shows that surface morphology of absorber layers deposited on the SLG. Facets and small sharp grains are present, in contrast to the smooth and large sharp grains deposited on the MoNa back contact. Moreover, there is a clearly observable difference in the morphology of the absorber layers on MoNa where the grain size increases as the thickness of the MoNa contact increases. The cross-sectional SEM images of all the absorber layers show a defined columnar structure, as can be seen in Figure 4. In observations of the absorber layers prepared on non-sodium substrates it is found that the columnar structure exhibits a uniform and large grain size from the surface to the back contact. However, the reduction in the grain size close to the interface between the absorber layers and back contacts may appear in layers with the addition of Na. This result is consistent with previous studies, in that the diffusivity of Ga is relatively lower [37]. At the same time, Ga-O and Na-O bonds form easily due to chemical electronegativity. The Ga diffusion is suppressed by the Na coming from the back contact to aggregate on the bottom [38]. Therefore, a non-homogenous Ga depth profile is revealed. The Raman spectra measured at the surface of absorber layers deposited on different back contacts are shown in Figure 5. The Raman spectra exhibited a single peak with no peak at 154 cm^{-1}, identified as belonging to the order vacancy compound, OVC), likely with $CuIn_2Se_{2.5}$, $CuIn_3Se_5$, $CuIn_5Se_8$ in the spectrum [34]. The main reason for the non-existence of the OVC peaks is that the intensity of the chalcopyrite band progressively becomes stronger, while the contribution from the OVC bands becomes negligible with a high copper ratio greater than 0.8 [35-36]. The Raman peaks of the absorber layers deposited on the SLG with MoNa back thicknesses of 0 nm, 100 nm, 200 nm are 171 cm^{-1}, 174 cm^{-1}, 174 cm^{-1} and 173 cm^{-1}, respectively. In principle, the shift in the peak can be attributed to chemical variation of the compound alloy occurring at the surface. It has been reported that the substitution of Na into Cu sites Na_{Cu} will result in the formation of a stable compound, $NaInSe_2$ [33]. It may be

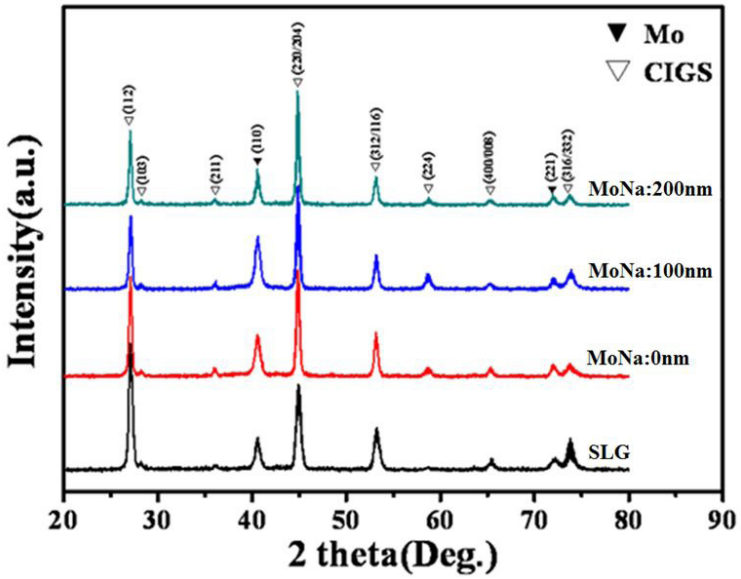

Figure 1: X-ray diffraction pattern of absorber layers with different back contact

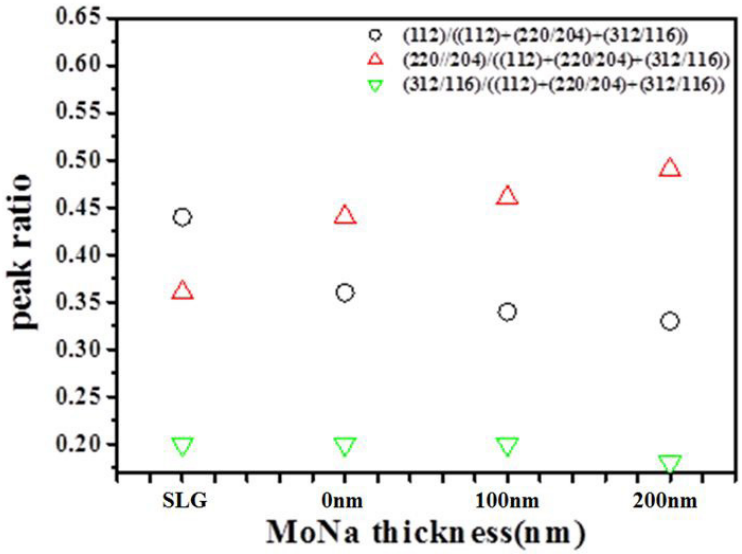

Figure 2: The peak ratio of (112), (220/204), and (312/116) of absorber layers with different back contact

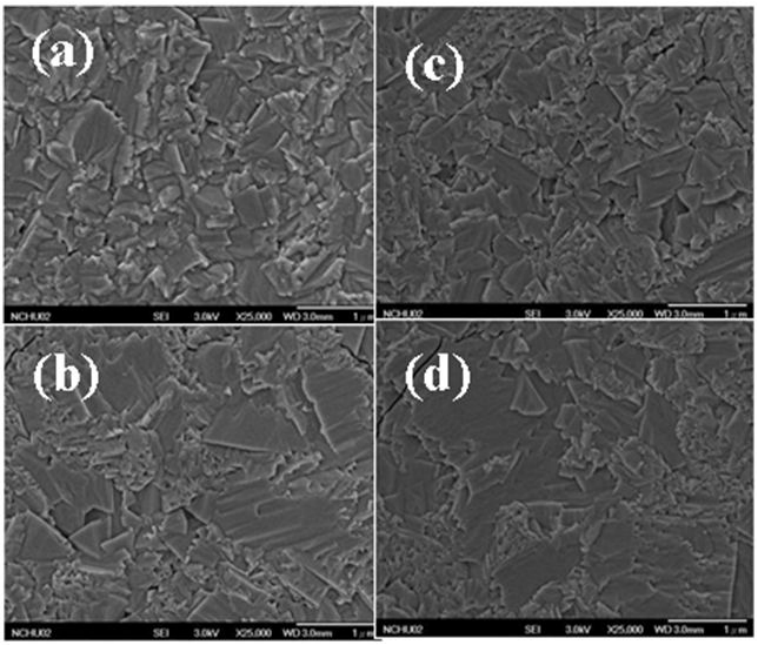

Figure 3: Plan-view SEM micrographs of CIGS film (**a**) SLG, (**b**) MoNa 0 nm, (**c**) MoNa 100 nm, (**d**) MoNa 200 nm

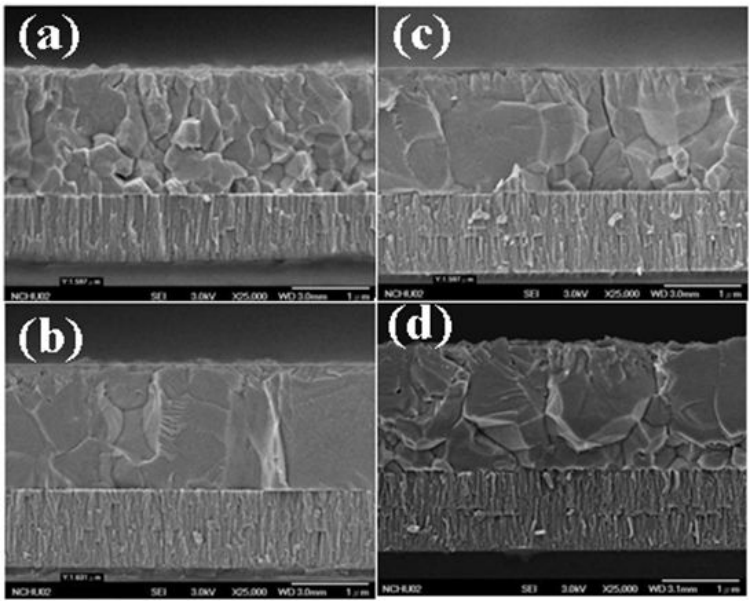

Figure 4: Cross-section SEM micrographs of CIGS film (**a**) SLG, (**b**) MoNa 0 nm, (**c**) MoNa 100 nm, (**d**) MoNa 200 nm

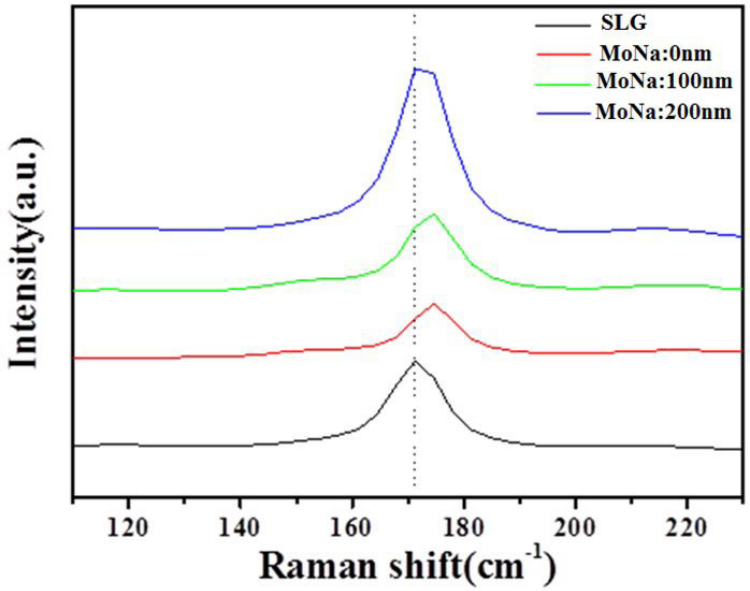

Figure 5: Raman spectra of absorber layers with different back contact

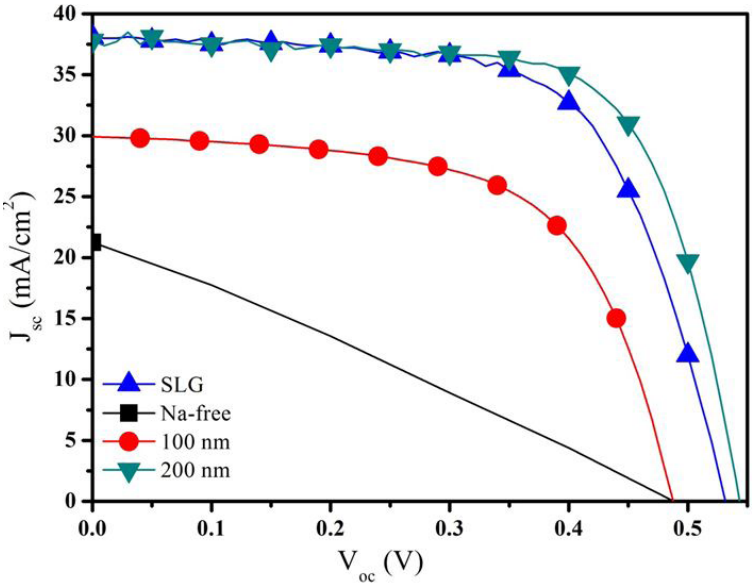

Figure 6: The I-V Characteristic of the solar cells with absorber layers deposited on SLG and different MoNa back contact thickness

demonstrated that a larger amount of Na contributing to the formation of $NaInSe_2$ at the surface can cause a Raman peak shift effect. The different absorber layers fabricated for thin film solar cells had the conventional Al-Ni/ZnO:Al/i-ZnO/CdS/CIGS/Mo/SLG structures. The efficiencies of solar cells with absorber layers deposited on SLG and MoNa backs with thickness of 0 nm, 100 nm and 200 nm are 13.71%, 2.71%, 8.98%, and 14.24%. The I-V characteristics of the solar cells with absorber layers deposited on SLG and MoNa back contacts with a thickness of 200nm are presented in detail, as shown in Figure 6. It is obvious that Na can improve the quality of the absorber layers as well as enhance the open-circuit voltage and fill factor of solar devices [11,12].

Conclusion

In this study, it is found that the choice of the proper Na content, so that there is a surfactant effect, is beneficial to (220/204) preferred orientation growth, instead of the (112) orientation. In other words, the excess Na content acts as an obstacle to growth. A reduction in the grain size near the back contacts appears, probably due to the suppression of Ga diffusion by Na. A larger amount of Na will replace Cu to form more $NaInSe_2$, causing a Raman peak shift effect. Finally, high conversion efficiencies of 13.71% and 14.24% are achieved by solar cells with absorber layers deposited on the SLG and MoNa back contact thickness of 200 nm, respectively.

References

1. Rockett A, Barkmire RM (1991) $CuInSe_2$ for photovoltaic applications. J Appl Phys 70: 81-97.

2. Orgassa K, Schock HW, Werner JH (2003) Alternative back contact materials for thin film Cu (In, Ga) Se_2 solar cells. Thin Solid Films 431: 387-91.

3. Gabor AM, Tuttle JR, Albin DS, Contreras MA, Noufi R, et al. (1994) High-efficiency $CuInxGa1-xSe_2$ solar cells made from $(Inx,Ga1-x)_2Se_3$ precursor films. Appl Phys Lett 65: 198.

4. Zhang SB, Wei SH, Zunger A, Katayama-Yoshida H (1998) Defect physics of the $CuInSe_2$ chalcopyrite semiconductor. Phys Rev B 57: 9642.

5. Nakada T, Kunioka A (1999) Direct evidence of Cd diffusion into $Cu(In,Ga)Se_2$ thin films during chemical-bath deposition process of CdS films. Appl Phys Lett 74: 2444.

6. Dullweber T, Hanna G, Rau U, Schock HW (2001) A new approach to high-efficiency solar cells by band gap grading in Cu (In, Ga)Se_2 chalcopyrite semiconductors. Sol Energy Mater Sol Cells 67: 145-50.

7. Dhingra A, Rothwarf A (1996) Computer simulation and modeling of graded bandgap CuInSe/sub 2//CdS based solar cells. IEEE Trans Electron Dev 43: 613-21.

8. Song J, Li SS, Huang CH, Crisalle OD, Anderson TJ (2004) Device modeling and simulation of the performance of Cu (In1−x, Gax) Se_2 solar cells. Solid-state Electronics 48 : 73-9.

9. Kessler F, Rudmann D (2004) Technological aspects of flexible CIGS solar cells and modules. Solar Energy 77: 685-95.

10. Otte K, Makhova L, Braun A, Konovalov I (2006) Flexible Cu (In, Ga) Se_2 thin-film solar cells for space application. Thin Solid Films 511-2: 613-22.

11. Hedström J, Ohlsén H, Bodegärd M, Kylner A, Stolt L, et al. (1993) ZnO/CdS/Cu(In,Ga)Se/sub 2/ thin film solar cells with improved performance. Conference Record of the 23th IEEE Photovoltaic Specialists Conf, Louisville : 364-71.

12. Ruckh M, Schmid D, Kaiser M, Schäffler R, Walter T, et al. (1996) Influence of substrates on the electrical properties of $Cu(In,Ga)Se_2$ thin films. Solar Ener Mater Solar Cells 41-42: 335-43.

13. Bodegärd M, Granath K, and Stolt L (2000) Growth of Cu (In, Ga) Se_2 thin films by coevaporation using alkaline precursors. Thin Solid Films 361-2: 9-16.

14. Rudmann D, Bilger G, Kaelin M, Haug FJ, Zogg H, et al. (2003) Effects of NaF coevaporation on structural properties of Cu (In, Ga) Se_2 thin films. Thin Solid Films 431-2: 37-40.

15. Chaisitsak S, Yamada A, Konagai M (2002) Preferred orientation control of Cu (In1-xGax) Se_2 (x≈0.28) thin films and its influence on solar cell characteristics. Jpn J Appl Phys 41: 507-13.

16. Rudmann D, da Cunha AF, Kaelin M, Kurdesau F, Zogg H, et al. (2004) Efficiency enhancement of $Cu(In,Ga)Se_2$ solar cells due to post-deposition Na incorporation. Appl Phys Lett 84: 1129-31.

17. Contreras MA, Egaas B, Dippo P, Webb J, Granata J, et al. (1997) On the role of Na and modifications to Cu(In,Ga)Se/sub 2/ absorber materials using thin-MF (M=Na, K, Cs) precursor layers [solar cells]. 26th IEEE PVSC Conf , USA.

18. Probst V, Rimmasch J, Riedl W, Stetter W, Holz J, et al. (1994) The impact of controlled sodium incorporation on rapid thermal processed Cu(InGa)Se/sub 2/-thin films and devices. Ist WCPEC Conf, USA.

19. Lundberg O, Lu J, Rockett A, Edoff M, Stolt L (2003) Diffusion of indium and gallium in Cu (In, Ga) Se_2 thin film solar cells. J Phys Chem Solids 64: 1499-504.

20. Contreras MA, Egaas B, Dippo P, Webb J, Granata J, et al. (1997) On the role of Na and modifications to Cu(In,Ga)Se/sub 2/ absorber materials using thin-MF (M=Na, K, Cs) precursor layers [solar cells]. 26th IEEE PVSC, USA.

21. Granath K, Bodegard M, Stolt L (2000) The effect of NaF on Cu (In, Ga) Se2 thin film solar cells. Sol. Energy Mater Sol Cells 60: 279-93.

22. Caballero R, Kaufmann CA, Eisenbarth T, Unold T, Schorr S, et al. (2009) The effect of NaF precursors on low temperature growth of CIGS thin film solar cells on polyimide substrates. Phys Status Solidi A 206: 1049-53.

23. Mansfield LM, Repins IL, Glynn S, pankow JW, Young MR, et al. (2011) Sodium-doped molybdenum targets for controllable sodium incorporation in CIGS solar cells. 37th IEEE PVSC, USA.

24. Klenk R, Walter T, Schock HW, Cahen D (1993) A model for the successful growth of polycrystalline films of $CuInSe_2$ by multisource physical vacuum evaporation. Adv Mater 5: 114-9.

25. Gabor AM, Tuttle JR, Albin DS, Contreras MA, Noufi R, et al. (1994) High-efficiency $CuInxGa1-xSe_2$ solar cells made from $(Inx,Ga1-x)_2Se_3$ precursor films. Appl Phys Lett 65: 198-200.

26. Gabor AM, Tuttle JR, Bode MH, Franz A, Tennant AL, et al. (1996) Band-gap engineering in Cu (In, Ga) Se_2 thin films grown from $(In, Ga)_2Se_3$ precursors. Sol Energy Mater Sol Cells 41-2: 247-60.

27. Granata JE, Sites JR, Asher S, Matson R (1997) Quantitative incorporation of sodium in CuInSe/sub 2/ and Cu(In,Ga)Se/sub 2/ photovoltaic devices. 26th IEEE PVSC, USA.

28. Matson RJ, Granata JE, Asher SE, Young MR (1998) Effects of substrate and Na concentration on device properties, junction formation, and film microstructure in $CuInSe_2$ PV devices. National Renewable Energy Laboratory, USA.

29. Niles DW, Ramanathan K, Hasoon F, Noufi R, Tielsch BJ, et al. (1997) Na impurity chemistry in photovoltaic CIGS thin films: Investigation with x-ray photo-electron spectroscopy. J Vac Sci Technol A 15: 3044-9.

31. Braunger D, Hariskos D, Bilger G, Rau U, Schock HW (2000) Influence of sodium on the growth of polycrystalline Cu (In, Ga)Se_2 thin films. Thin Solid Films 361-2: 161-6.

30. Bodegard M, Stolt L, Hedström J (1994) The influence of sodium on the grain structure of CuInSe_2 films for photovoltaic applications. Proce 12th Euro Photovoltaic Solar Energy Conf 1743-6.

32. Herberholz R, Rau U, Schock HW, Haalboom T, Godecke T, et al. (1999) Phase segregation, Cu migration and junction formation in Cu(In, Ga)Se_2. Eur Phys J AP 6: 131-9.

33. Wei SH, Zhang SB, Zunger A (1999) Effects of Na on the electrical and structural properties of $CuInSe_2$. J Appl Phys 8: 7214-8.

34. Xu CM, Xu XL, Xu J, Yang XJ, Zuo J, et al. (2004) Composition dependence of the Raman A1 mode and additional mode in tetragonal Cu–In–Se thin films. Semicond Sci Technol 19: 1201-6.

35. Papadimitriou D, Esser N, Xue C (2005) Structural properties of chalcopyrite thin films studied by Raman spectroscopy. Physica status Solidi B 242: 2633-43.

36. Fontané X, Izquierdo-Roca V, Calvo-Barrio L, Álvarez-García J, Pérez-Rodríguez A, et al. (2010) Investigation of compositional inhomogeneities in complex polycrystalline Cu(In,Ga)Se_2 layers for solar cells. Appl Phys Lett 95: 121907.

37. Wagner S, Bridenbaugh PM (1997) Multicomponent tetrahedral compounds for solar cells. J Cryst Growth 39 :151-9.

38. Ruckh M, Schmid D, Kaiser M, Schäffler R, Walter T, et al. (1996) Influence of substrates on the electrical properties of Cu (In, Ga)Se_2 thin films. Sol Energy Mater Sol Cells 41-2 : 335-43.